*Journal of Sound and Vibration* (1999) **220**(3), 541–557
*Article No*. jsvi.1998.1972, available online at http://www.idealibrary.com on IDEAL

# CONTROL OF AIRCRAFT INTERIOR BROADBAND NOISE WITH FOAM-PVDF SMART SKIN

C. GUIGOU† AND C. R. FULLER

*Vibration and Acoustics Laboratories, Mechanical Engineering Department, Virginia Polytechnic Institute and State University, Blacksburg, VA* 24061-0238, *U.S.A.*

(*Received* 10 *October* 1997, *and in final form* 9 *September* 1998)

A foam-PVDF smart skin design for aircraft interior noise control is discussed. The smart skin is designed to reduce sound by the action of the passive absorption of an acoustic foam (which is effective at higher frequencies) and the active input of a PVDF element driven by an oscillating electrical input (which is effective at lower frequencies). For performance testing, the foam-PVDF smart skin is mounted in the cockpit of a Cessna Citation III fuselage. The fuselage crown panels are excited with a speaker located on the outside of the cockpit and driven by a band-limited random excitation. A MIMO feedforward Filtered-x LMS controller is implemented to minimize the error sensor signals provided by microphones in the close proximity of the smart skin elements. Three different reference signals are implemented for the feedforward controller and are compared in terms of the interior noise attenuation achieved. The voltage sent to the disturbance speaker provides an optimal reference signal which is not realistic in practice. Thereore, the use of either a structural sensor (accelerometer directly mounted on the fuselage) or an acoustic sensor (microphone located close to the fuselage) is investigated to supply a practical reference signal. The potential of the smart foam-PVDF skin for reducing interior noise is demonstrated.



## 1. INTRODUCTION

In the last decade, many research studies have been dedicated to reducing interior noise of aircraft. Noise fields generated by turbofans, propellers and turbulent boundary layer for example, impinge on the exterior of the fuselage and induce large sound levels inside the cabin of aircraft. Two main active control methods have been widely investigated to reduce low frequency sound transmission in aircraft [1–5]. Active Noise Control (ANC) consists of adding secondary acoustic sources (most commonly loudspeaker) inside the aircraft fuselage [6]. These secondary sources are used to minimize sound pressure levels by reducing signals from error microphones usually located close to passenger head height. Active Structural Acoustic Control (ASAC) involves secondary structural input (either mechanical shakers or piezoelectric ceramic actuators) applied directly to the

† Currently at C.S.T.B., 24 rue Joseph Fourier, 38400 St Martin d'Hère, France.

0022–460X/99/080541 + 17 $30.00/0 

aircraft [7]. In this case, the control actuators are used to decrease either microphone signals or structural information measured on the fuselage that is related to sound radiation. Although good performance is often obtained, localized sound attenuation, control spill-over and the inability to obtain high frequency sound reduction are some of the drawbacks associated with both the ANC and ASAC approaches. On the other hand, the use of passive materials such as damping visco-elastic material, added mass and porous layer can be considered for reducing sound radiation. However, such a passive technique is not very efficient in the low-frequency region. The complementary nature of passive and active noise control techniques can be used to develop hybrid devices for control over extended frequency range [8]. Indeed, in the last few years, there has been an increased interest in the reduction of sound and/or vibrations by use of hybrid active-passive control techniques. The passive device usually carries the primary attenuation function, while the active component is used to enhance the passive system performance or overcome the limitations of the passive system. This work is concerned with testing an active-passive surface coating in order to attenuate sound radiation that an untreated surface would otherwise generate due to its vibrations. Indeed, such coating can be used, for example, to reduce aircraft cabin noise due to an exterior turbulent boundary layer. The eddies of the turbulent flow cause the outer aluminum skin to vibrate as shown in Figure 1. Aircraft cockpit, or cabin noise has definite negative effects on speech interference (pilot to pilot and pilot to air-traffic controller) as well as being a critical factor in increasing mental fatigue. The active–passive surface coating concept is to completely cover the inner surface of the aircraft skin with contiguous independent active tiles. When the radiation impedance is driven to zero, no sound is radiated inside the fuselage (see Figure 1). The active–passive surface coating developed in this work is implemented in the cockpit of the mid size business jet Cessna Citation III located at VPI&SU. Here, it is of interest to control cockpit noise due to a

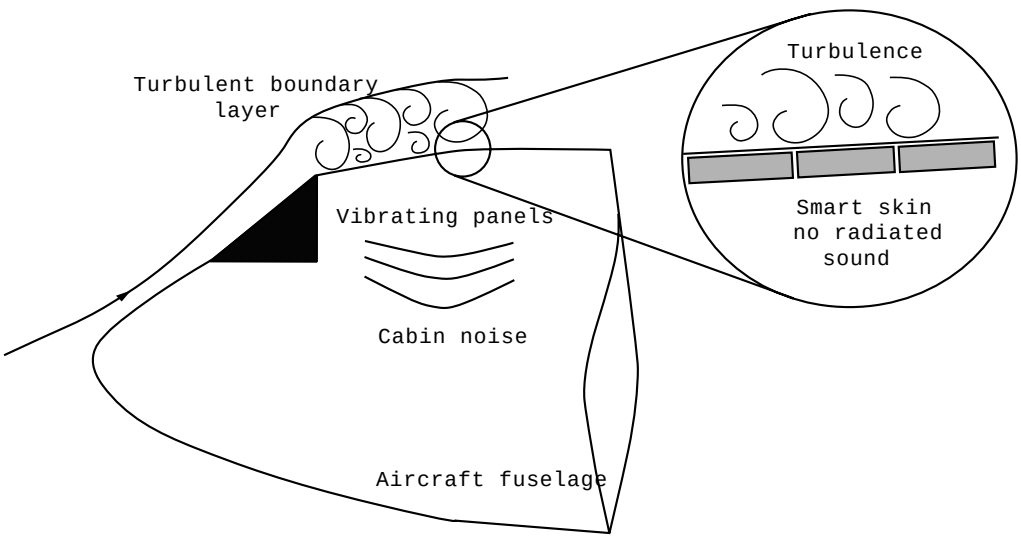


Figure 1. Schematic of the system.

localized flow separation and associated turbulence over the crown of the aircraft as shown in Figure 1.

Porous sound-absorbing materials are commonly implemented for a large range of applications (such as buildings, machinery enclosures and aircrafts) to reduce sound propagation and transmission [9, 10]. For passive sound absorbers, the air molecules in the interstices of the porous material oscillate with the frequency of the exciting sound wave. These oscillations result in frictional losses. Changes in flow direction and expansions and contractions of the flow throughout irregular pores result in a loss of momentum in the direction of wave propagation. For example, a porous layer can absorb a large amount of acoustic energy if its thickness is comparable to a quarter of the wavelength of the incident sound [10]. Bolton and Green [11] presented an analysis demonstrating that the low frequency performance of a finite-depth layer of elastic porous material may be enhanced by applying an appropriate force to the solid phase at the front surface of the layer. They showed that at any angle of incidence, the solid phase of the foam may be forced so as to create a perfect impedance match with the incident plane wave, thus causing the sound to be completely absorbed. However, no physical implementation of such a devise was discussed. In connection with this, Fuller *et al*. [12] outlined a "smart foam" to be used as active–passive sound absorber that can be obtained by incorporating piezoelectric materials within the foam layer. The piezoelectric PVDF element serves as the active input to contribute to the low frequency sound attenuation. It is cylindrically curved to couple the in-plane strain associated with the piezoelectric effect with the vertical motion needed to radiate sound from the foam surface. The smart foam can be bonded directly to a vibrating structure and acts as an active surface coating that provides reduction of structural sound radiation. It is expected that the smart foam can modify the acoustic impedance seen by the structure in order to yield a net decrease in the sound power radiated by the vibrating noise source. The potential of the smart foam to simultaneously control low and high frequency sound, has been demonstrated on a simple radiating source (piston) [13, 14]. Global cancellation of harmonic and broadband noise, induced by a vibrating piston was successfully achieved by the smart foam. The passive–active device was able to modify the radiation impedance observed by the piston over a wide range of frequencies. Recently, the use of multiple smart foam modules (with a MIMO control system) was also investigated to reduce the sound radiation from a complex radiating source (an elastic plate) [15]. These works provided the basis of the present study.

In this paper, the foam-PVDF smart skin is mounted in the cockpit of a Cessna Citation III fuselage. Each smart skin element controls the effective acoustic source of the fuselage panel it is mounted on. The fuselage is excited with a speaker located on the outside of the cockput to simulate the acoustic source of the flow separation. The signal driving the speaker is band-limited and random. A MIMO feedforward Filtered-x LMS controller [6] is implemented to minimize the error sensor signals provided by microphones in the close proximity of the active elements. Three different reference signals are implemented for the feedforward controller and are compared in terms of the interior noise attenuation achieved. The voltage sent to the disturbance speaker provides an optimal reference signal

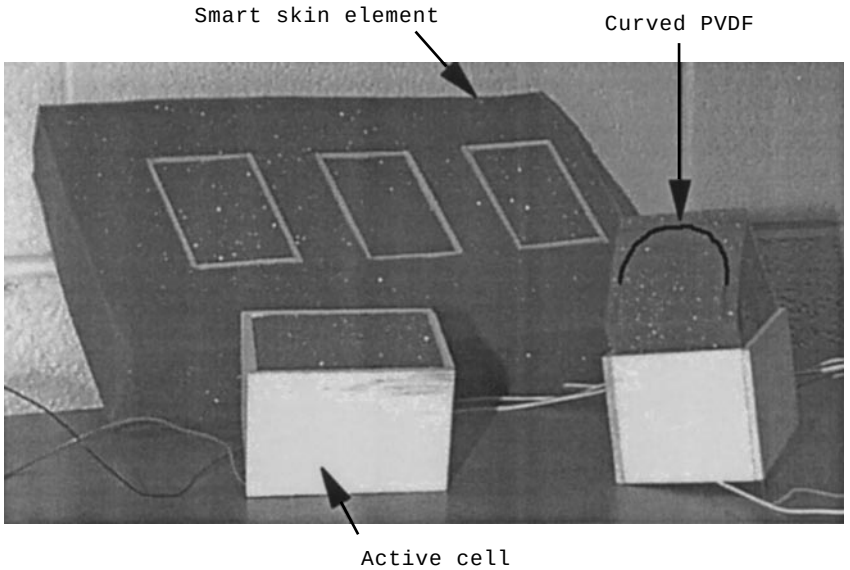


Figure 2. Smart foam.

which is not realistic in practice. Therefore, the use of either a structural sensor (accelerometer directly mounted on the fuselage structure) or an acoustic sensor (micropohone located close to the fuselage) is investigated to supply a practical reference signal. The potential of the smart foam-PVDF skin for reducing interior noise is discussed.

## 2. SMART FOAM DESCRIPTION

A sound-absorbing material, known as partially-reticulated polyurethane foam, provides the passive element of smart foam. Such material dissipates incident acoustic wave energy through friction associated with the coupling of the liquid and solid phases of the foam. Partially-reticulated polyurethane foam is an acoustical grade, open cell, flexible ester based urethane foam designed to give maximum sound absorption per given thickness [16]. Since passive sound control is only significant at high frequencies, a 28 μm Ag metallized PVDF film is embedded in the foam to implement the active control, which is most effective at low frequencies. A silver-electroded PVDF was chosen, as it can sustain high voltage amplitudes required for actuator applications. The main physical characteristic of the PVDF actuator is that it is intentionally curved to couple the predominantly in-plain strain associated with the piezoelectric effect and the vertical motion that is required to accelerate fluid particles and hence radiate sound away from the surface of the foam. Much work has been done to investigate the optimal configuration of the components of the smart foam. The PVDF film is curved into a half-cylinder of 1·5 in. diameter and 2·5 in. long (see Figure 2) and is embedded in two foam halves with spray glue. This leads an "active cell" which is 3 in. long, 2 in. wide and 2 in. thick as depicted in Figure 2. Note that the active cell is encased in a thin balsa wood frame for improved radiation

efficiency [15]. Each smart skin element is composed of three active cells (see Figure 2) driven in phase, and is then mounted on a fuselage crown panel.

## 3. CONTROL EXPERIMENTAL SETUP

Four crown panels were treated with the smart skin as Figure 3. Each treated crown panel corresponds to a control channel (C1–C4). As mentioned previously, each control channel is associated with three active cells driven in phase. Four error microphones were located at pilot's ear level (about 7 in. below the cockpit fuselage ribs). Band-limited and broadband random excitation (simulating the excitation of the flow separation and associated turbulence) of the crown panels is achieved with a speaker mounted on the outside of the cockpit. The disturbance speaker was located at the center of the treated area, about 1 in. from the fuselage structure above the top ribs (see Figures 3 and 4). A traverse composed of 12 microphones (1·5 in. apart) was used to monitor the performance of the control in the planes located at pilot's ear and shoulder level (approximately 7 and 14 in. below cockpit ceiling). The traverse was moved by a step of 2 in. in each measurement plane, which covered the area under the four treated fuselage crown

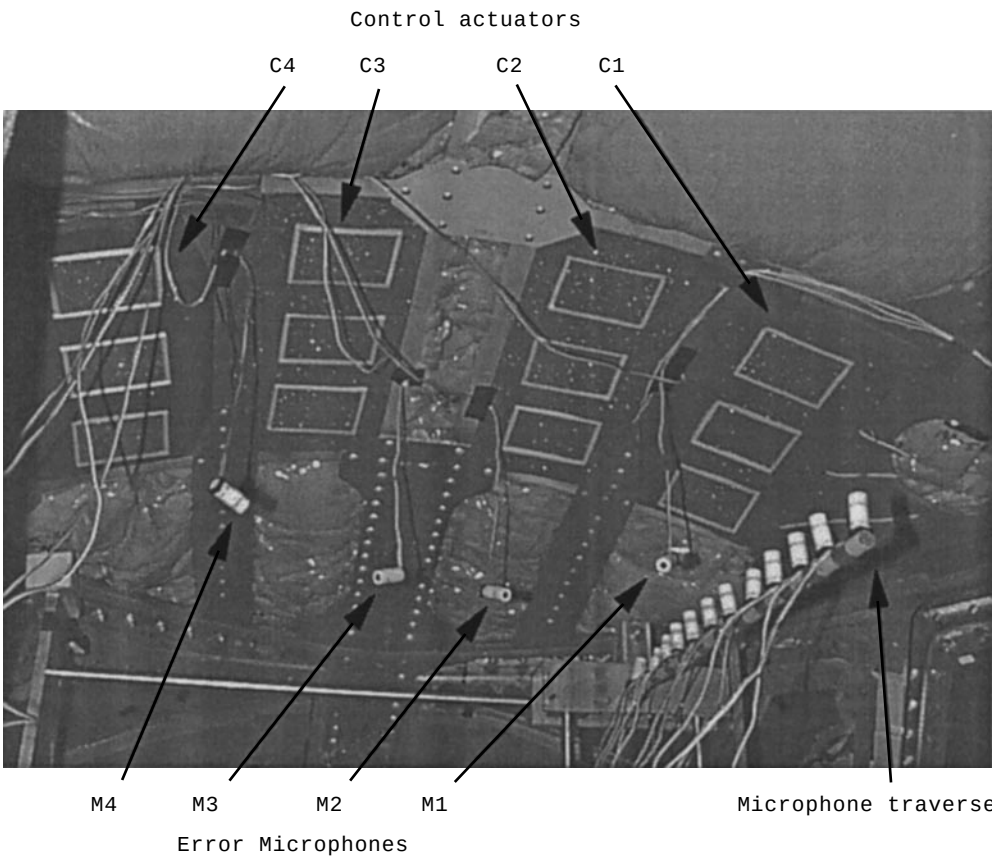


Figure 3. Cessna crown panels control arrangement.

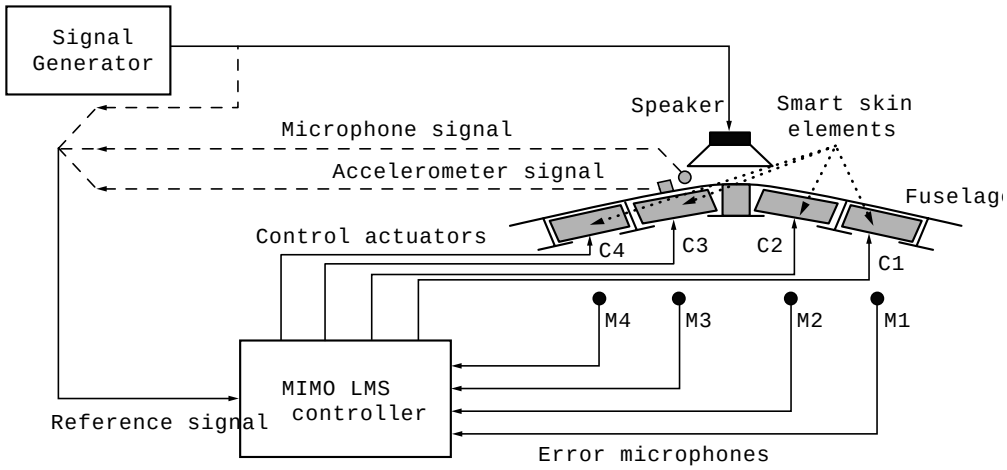


Figure 4. Schematic of control set-up.

panels (see Figure 3). Thus, 108 sound pressure levels (SPL) were recorded in each measurement plane (i.e., at pilot's ear and shoulder level). The global attenuation associated with the control in each measurement plane was calculated as the ratio of the sum of the 108 measured square pressures summed over the excitation frequency range, before and after control. A MIMO feedforward Filtered-x LMS algorithm [6, 7] implemented on a TMS320 C40 DSP was used to determine the appropriate control signals necessary to minimize the acoustic pressure at the error microphones. Either the signal sent to the disturbance speaker, the signal from an accelerometer directly mounted on the fuselage section under the excitation or the signal from a microphone located close to the fuselage (last two signals being more realistic in practice) is used as reference signal for the controller. Note that, at the time of the experiments, a surface mounted microphone was not available; for this reason, a simple microphone was suspended closely above to the fuselage surface to provide a reference signal. If such a microphone reference sensor provides a good control strategy, a surface mounted microphone would have to be implemented in a practical test. Results for the different reference signals are compared in terms of the interior noise attenuation achieved. Figure 4 presents a schematic of the control set-up. The controller used a sampling frequency of 2·8 kHz; 90 and 100 coefficient FIR filters were implemented for the error and control paths respectively. Note that when the accelerometer or the microphone signal is the reference signal, the effect of the control actuators on this signal was not taken into account (feedback removal) [6], as it was found to be negligible.

The passive effect of the four smart skin elements was first investigated. The SPL's at the four error microphones and in the pilot's ear level plane as well as the displacement at the accelerometer were measured without and with the four smart skin elements mounted in the crown panels. The passive effect of the smart foam was found to be limited to the resonance frequencies of the fuselage crown panel mainly in the form of additional vibration damping. It is interesting to observe, however, that acoustic foam can be used as an effective *vibration* damper by attaching it to the structural surface. In average, 4 dB passive sound attenuation

was obtained at pilot's ear level in the frequency range 250–1250 Hz, which is still significant.

## 4. CONTROL RESULTS

### 4.1. COMPARISON BETWEEN 2 AND 4 CONTROL CHANNEL SYSTEMS

A 250–1050 Hz broadband random signal is sent to the exterior speaker exciting the crown panels. This signal is used as the controller reference signal. Either 2 or 4 control channels are implemented. In the 2 control channel case, only error microphones M1 and M4, and smart skin elements C1 and C4 (see Figures 3 and 4) are used by the controller. Figure 5 presents the attenuation achieved at the different error microphones. It can be seen that the SPL's at error microphones M2 and M3 are only slightly reduced, when the 2 control channel system is implemented, since these signals are not directly minimized by the control. On the other hand, the attenuation at error microphones M1 and M4 is larger for the 2 control channel system than for the 4 channel one. As expected, the 4 control channel system is associated with very good attenuation at all four error microphones. Figure 6 presents the global attenuation obtained in pilot's ear level plane. The advantage of using a 4 control channel system is clear, as the SPL's are very well reduced in the entire measurement plane. Indeed, for the 2 control channel system, the pressure field is only reduced in the close proximity of the two error microphones (i.e., M1 and M4) minimized by the controller. The global attenuation associated with active control is then only of 2·5 dB for the 2 control channel system, while it is 8 dB for the 4 control channel system. These results demonstrate that increasing the number of channels from 2 to 4 greatly improves the global performance of the control by increasing the area of attenuation. In the

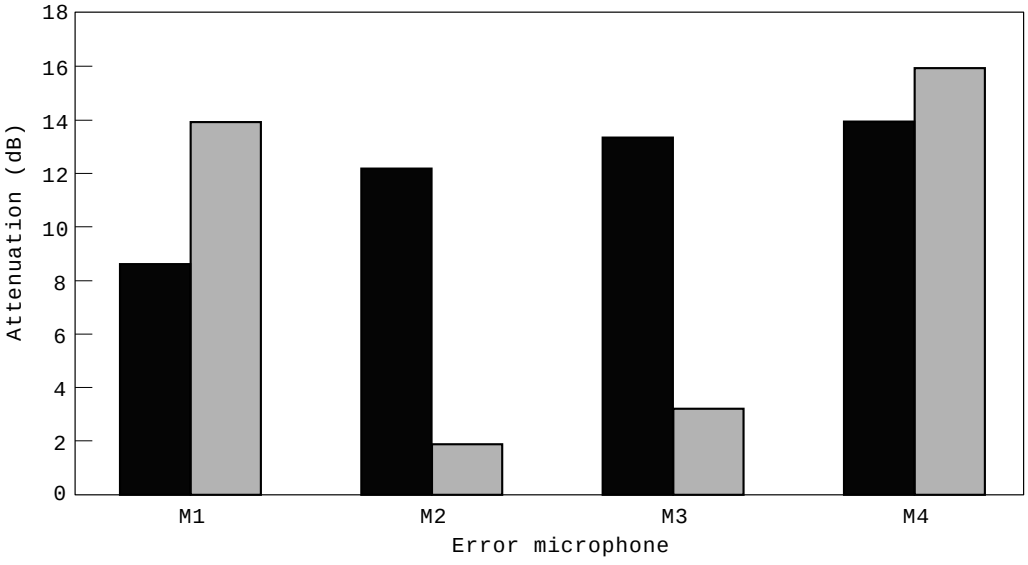


Figure 5. Attenuation at error microphones for ■ 4 and □ 2 control chennel system.

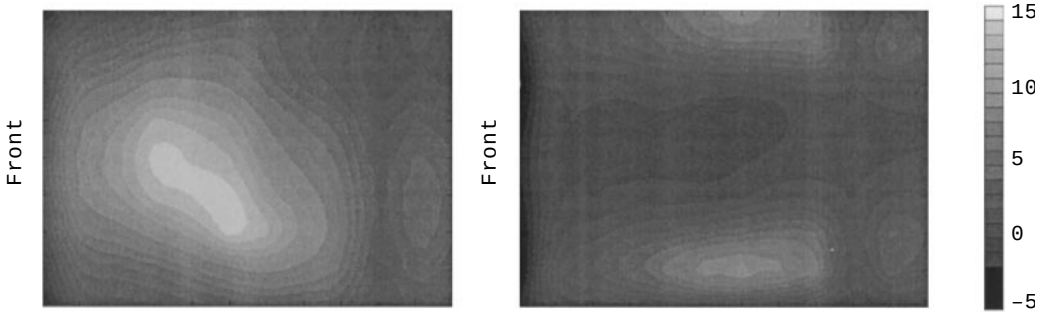


Figure 6. Attenuation in pilot's ear level plane for (a) 4 and (b) 2 control channel system.

following results, the MIMO control system is implemented with 4 control channels (i.e., 4 error microphones M1–M4 and 4 smart skin elements C1–C4).

### 4.2. COMPARISON BETWEEN DIFFERENT ERROR MICROPHONE LOCATIONS

In this section, four error microphones are used. Their location is varied and the effect on the control performance is investigated. The signal sent to the exterior speaker exciting the crown panels is random with a frequency bandwidth of 250–1050 Hz. This signal is used as the controller reference signal. In the first configuration, the error microphones are located about 7 in. below the top fuselage ribs and in front of the center active cell of each smart skin element. The second configuration is depicted in Figure 3. The error microphones are still positioned 7 in. below the top fuselage ribs but are no longer aligned. Indeed, the idea behind this configuration is to shape the attenuation zone in the ear level plane such that the pilot could move his/her head forward and still experience low noise level. The third configuration is similar to the first one but the error microphones are moved closer to the foam, about 3 in. below the top fuselage ribs. For the first and third configuration, the error microphones are aligned. Figure 7 presents the attenuation obtained for the three different error microphone configurations in the pilot's ear level plane. Configuration 1 leads to an averaged attenuation of 8 and 6 dB in the pilot's ear and shoulder level plane respectively. In this case, the area of important attenuation ($>10$ dB) is found as expected along the line described by the error microphones [see Figure 7(a)]. When the microphones are moved closer to the smart skin elements (i.e., configuration 3), the averaged attenuation is decreased to 6 dB in the pilot's ear and shoulder plane. As seen in Figure 7(c), the region of important attenuation ($>10$ dB) is reduced and no longer follows the line described by the error microphones (since the error microphones are not in the measurement plane). The attenuation achieved when the error microphones are in configuration 2 can be seen in Figure 7(b). The area of important attenuation ($>10$ dB) is moved towards the front of the measurement plane as planed. The achieved averaged attenuation is 8 dB in the pilot's ear plane and 6·4 dB in the pilot's shoulder plane. Therefore, the global control performance in both measurement planes is very similar for configurations 1 and 2. However,

configurations 1 and 2 correspond to different regions of large attenuation at the pilot's ear level. In the following results, either configuration 1 or 2 is implemented.

### 4.3. BAND-LIMITED CONTROL RESULTS 500–700 Hz

In this section, the error microphones are placed in configuration 1. The signal sent to the speaker exciting the crown panels is random and band-limited between 500 and 700 Hz (200 Hz bandwidth). Three different reference signals for the control algorithm: the signal sent to the disturbance speaker, the signal from an accelerometer directly mounted on one of the crown panels or the signal from a microphone located close to the fuselage (see Figure 4), are investigated.

Figure 8 presents the SPL at the error microphones before control and under the three different control conditions. The total attenuation at the four error microphones is shown in Figure 9. It can be seen that the SPLs at the error microphones are very well reduced when the speaker signal is used as reference. More than 15 dB averaged attenuation is achieved at each of the error microphones. When the referrence signal is obtained from the accelerometer mounted on the crown panel, the error microphone signals are not as well decreased (around 6 dB attenuation in average). Note that the effect of the smart skin elements (control actuator) on the accelerometer signal was very limited (no feedback); this means that the vibrational levels of the fuselage were not considerably increased during control. It can be seen in Figures 8 and 9 that the controller using a microphone as reference sensor performs much better than that

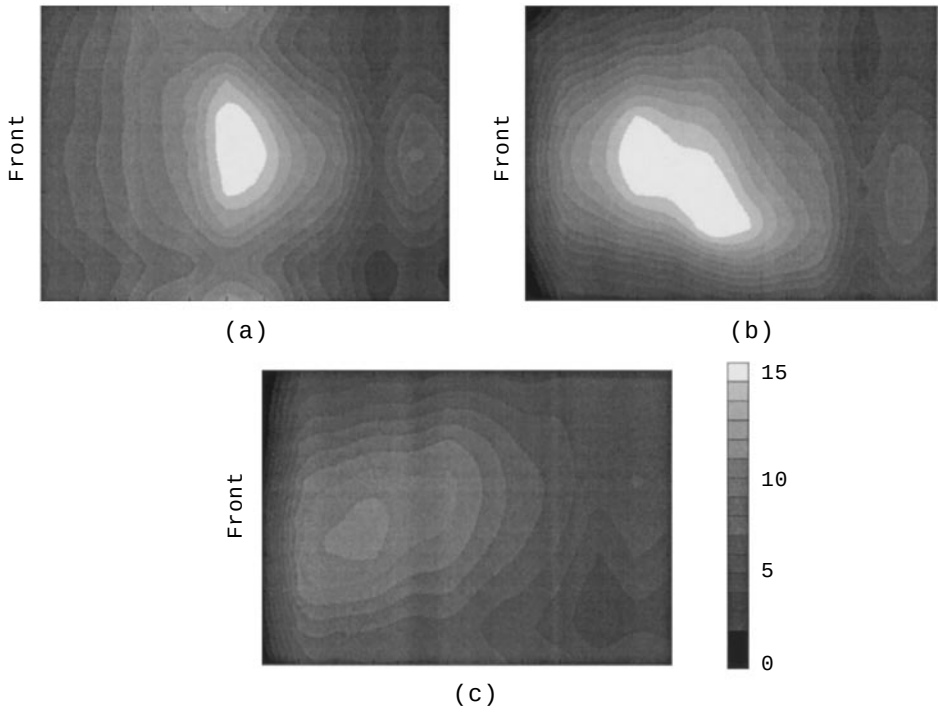


Figure 7. Attenuation in the pilot's ear level plane for the error microphones in (a) configuration 1, (b) configuration 2 and (c) configuration 3.

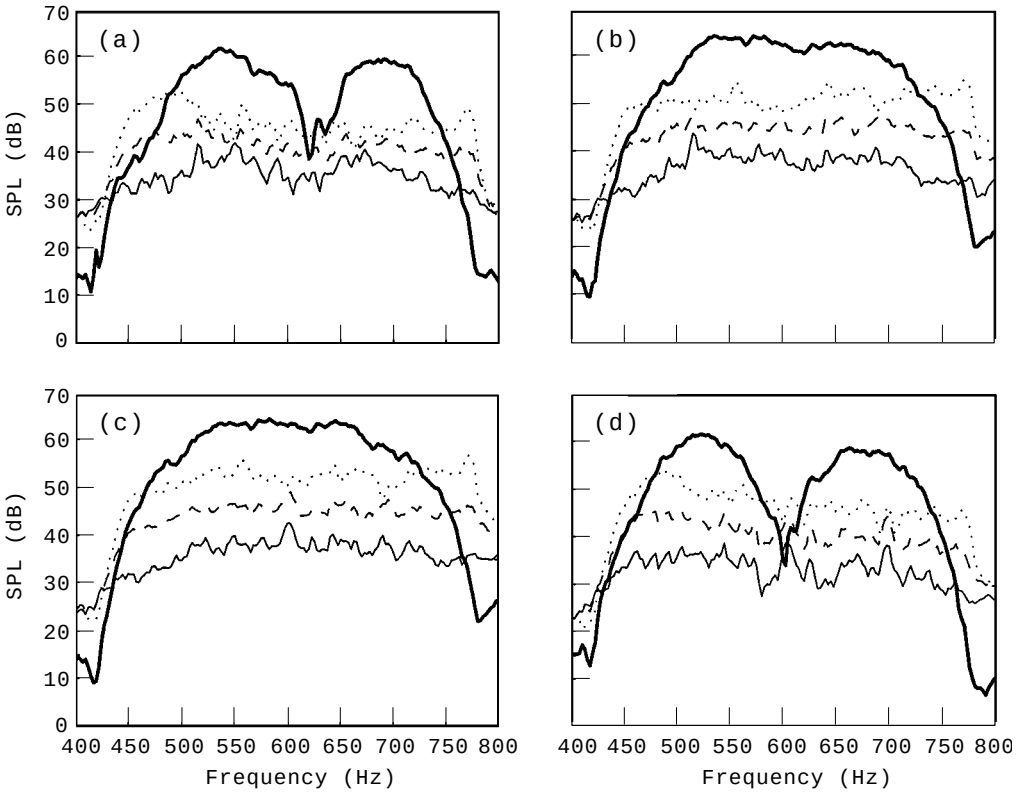


Figure 8. SPL at error microphones (a) M1, (b) M2, (c) M3 and (d) M4. ——, Before control; ——, speaker signal as reference; · · · · ·, accelerometer signal as reference; – – –, microphone signal as reference.

using a structural accelerometer. When using the microphone to provide a reference signal to the feedforward control, the error microphone signals are decreased by more than 10 dB in the frequency range studied. Figure 10 presents the global attenuation in the pilot's ear level plane for the three different control conditions. When the reference signal is the speaker signal, large attenuation is obtained along the line described by the error microphones. This results in a global active attenuation of 12·5 dB in the pilot's ear plane and 10 dB in the pilot's shoulder plane. When the reference signal is the accelerometer signal, the attenuation is nearly constant throughout the pilot's ear level plane [see Figure 10(b)] as well as the pilot's shoulder level plane. Indeed, a global active attenuation of 6·5 and 6·2 dB is obtained at pilot's ear level, which also results in more than 5·5 dB global attenuation at pilot's shoulder level. Using a microphone located close to the fuselage surface to apply the reference signal to the feedforward controller yield good global attenuation, about 9 dB at pilot's ear level and 7·5 dB at pilot's shoulder level. However, as shown previously, the passive action of the skin provides around 4 dB attenuation. Thus, the total attenuation due to the active–passive skin is approximately 10 dB with a realistic reference signal. Thus, using a realistic reference signal still yields very appreciable attenuation at pilot's ear level.

The difference in control performance between the unrealistic (signal to disturbance speaker) and practical (signal from the accelerometer or microphone) reference signals can be associated to two facts. Either the reference signal is not coherent with the error signals, and/or the propagation time through the control path is too long compared to the propagation time through the disturbance path. Here, the propagation time through the control path is defined as the time for signal to propagate from the D/A output DSP board to the control actuators and to the error microphones (this path includes anti-aliasing filters, power amplifiers, and error microphone signal conditioning amplifier). On the other hand, the propagation time through the disturbance path is defined as the time delay between the reference signal (to be input to the A/D input DSP board) and the error microphones (this path includes a signal conditioning amplifier depending on the reference signal implemented and error microphone signal conditioning amplifier). Indeed, the controller must be able to receive the reference signal, and produce the appropriate control signals to the smart skin elements, before the acoustic disturbance from the speaker propagates from the fuselage outer skin past the foam. In other words, the poor control performance achieved with realistic reference sensors can be due to coherence and/or causality problems. To investigate these two possibilities, the fuselage was excited with a random noise between 250 and 1050 Hz. The coherence between the different reference sensors and different error microphones was first measured. Figure 11 presents the coherence between the three reference signals and error microphone M2 (which was found to be representative of the coherence measurements). For any of the reference signals, the coherence is close to 1 for the entire frequency range. Therefore, the lack of coherence is not the reason for the low control performance observed with the realistic reference signals. The system causality was studied next.

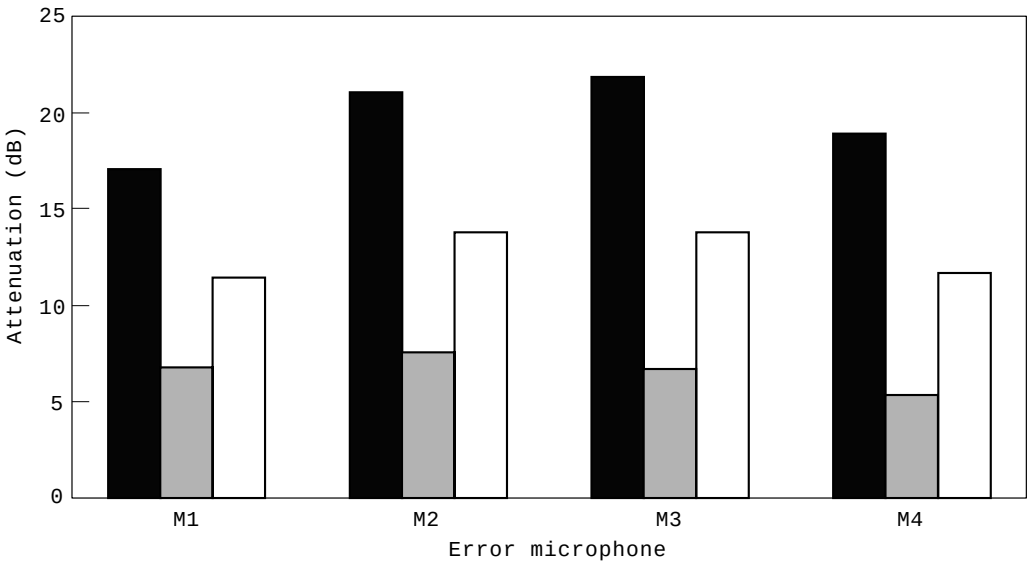


Figure 9. Attenuation at error microphones for band-limited 500–700 Hz excitation; ■, speaker as reference; ▒, accelerometer signal as reference; □, microphone signal as reference.

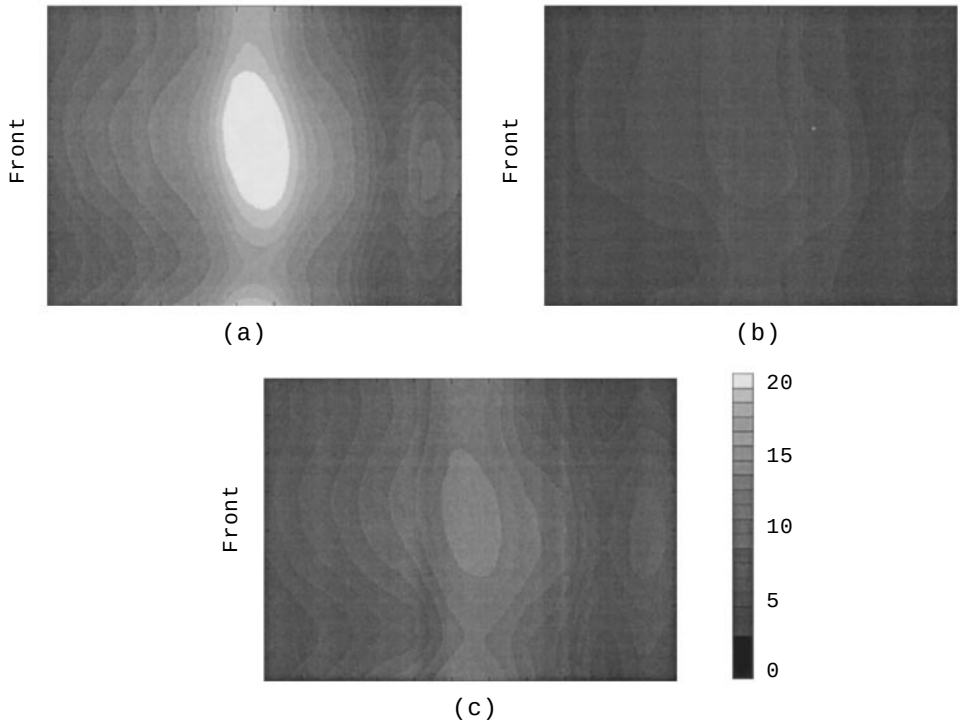


Figure 10. Attenuation in the pilot's ear level plane for band-limited 500–700 Hz excitation; with reference as (a) speaker signal, (b) accelerometer signal and (c) microphone signal.

To this end, the cross-correlation was measured for the different cases of interest and the corresponding time delays were deduced [17]. Table 1 shows the time delay or propagation time associated with the different disturbance paths (i.e., different reference signals to the signal from error microphone M2 signal) as well as the control path (between the signal sent to smart foam element C2, and the signal from error microphone M2). As expected, the propagation time through the disturbance path is reduced when the reference signal is changed from the speaker signal to the accelerometer or microphone signal. Then, the time delay for the controller to react is much shorter when the reference signal is from the accelerometer directly mounted on the fuselage or the microphone located close to the fuselage than when it is the signal driving the speaker. However, the propagation time through the disturbance path associated with the accelerometer signal is much shorter than that of the reference microphone signal. The time propagation of the control path is shorter than the propagation time through the disturbance path, when the reference signal is either the disturbance speaker signal or the reference microphone signal. This means that such control systems are causal. On the other hand, the propagation time through the control path is longer than the propagation time through the disturbance path when the accelerometer signal is used as reference signal. Therefore, the control system is acausal, which explains the low control performance achieved in this case. Note that the short propagation time associated with the accelerometer is believed to be related to the

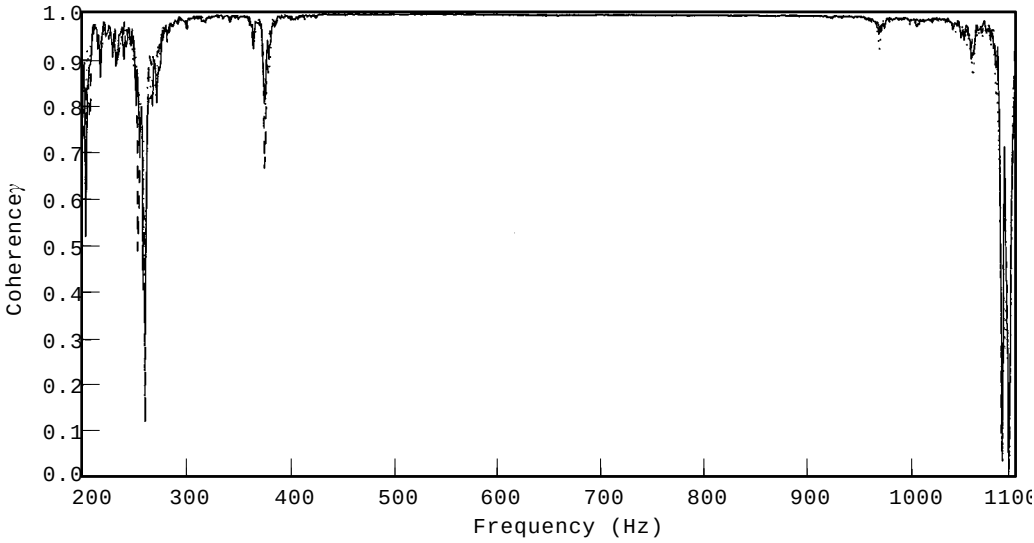


Figure 11. Coherence between the different reference signals and error microphone M2; ——, speaker signal as reference, · · · · ·, accelerometer signal as reference; – – –, microphone signal as reference.

type of accelerometer and charge amplifier (slow response) available for the experiments (B&K brand). Other types should be investigated in the next future in order to improve the control results.

### 4.4. BAND-LIMITED CONTROL RESULTS 500–900 HZ

In this section, the error microphones are placed in configuration 3. The signal sent to the speaker exciting the crown panels is random and band-limited between 500 and 900 Hz (400 Hz bandwidth). The three different reference signals as previously described are again considered for the control implementation and compared in terms of control performance. Figure 12 presents the attenuation at the error microphones for the three different control conditions. As in the previous case, the SPLs at the error microphones are best reduced when the speaker signal is used as reference. More than 15 dB averaged attenuation is achieved at three of the error microphones in this case. When the reference signal is obtained from the accelerometer mounted on the crown panel, the error microphone signals are

TABLE 1

*Propagation time measurements*

| Signal path | Description | Propagation time (ms) |
|---|---|---|
| Disturbance path | Speaker to error microphone M2 | 2·5 |
| | Accelerometer to error microphone M2 | 0·4 |
| | Reference microphone to error microphone M2 | 2·0 |
| Control path | Smart foam element C2 to error microphone M2 | 1·0 |

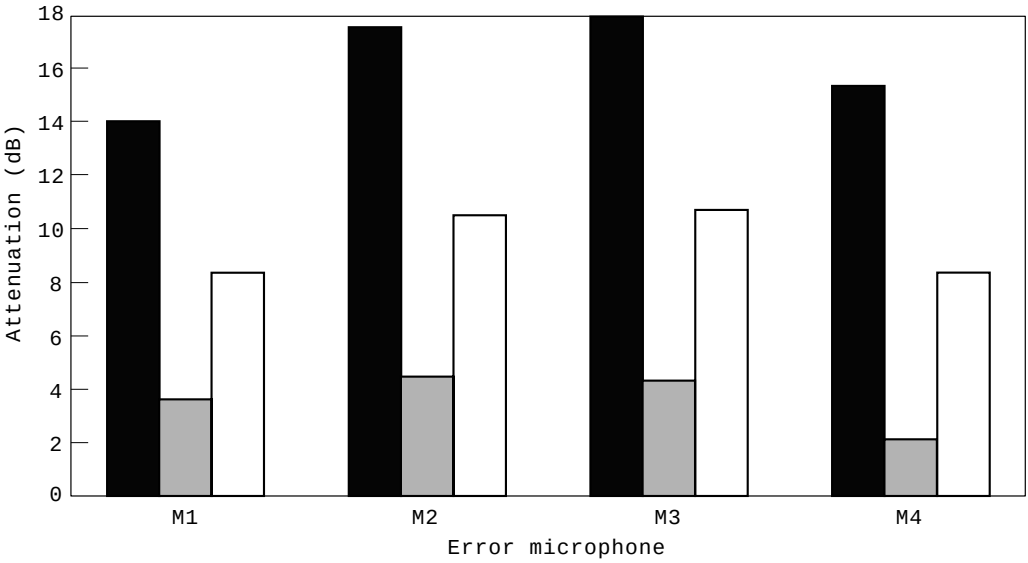


Figure 12. Attenuation at error microphones for band-limited 500–900 Hz excitation; ■, speaker as reference; ▩, accelerometer signal as reference; □, microphone signal as reference.

not as well decreased ($<5$ dB attenuation in average). Using the signal from the microphone located close to the fuselage as reference signal yields a decrease of more than 8 dB at all four error microphones. The control results are again better when using the microphone sensor than when using the accelerometer as reference sensor. Furthermore, as the frequency bandwidth is increased, the control performance is decreased in average, especially in the case where the accelerometer is used to provide a reference signal to the controller. A global active attenuation of 8 dB is achieved in the pilot's ear level plane when the speaker signal is used as reference signal. The global active attenuation is reduced to 5 or 2·5 dB when the microphone or accelerometer provides the reference signal respectively. As explained previously, this reduced control performance is associated with the shorter time delay for the controller to react when the accelerometer provides the reference signal. Including the passive action of the skin (around 4 dB attenuation), the total attenuation due to the active–passive skin is about 9 dB with a realistic reference signal (microphone), which is still a very good performance.

### 4.5. BROADBAND CONTROL RESULTS 250–1050 HZ

In this section, the error microphones are again placed in configuration 3. The excitation is a 800 Hz bandwidth random signal (250–1050 Hz of frequency range). The three different reference signals as previously described are again considered for the control implementation and compared in terms of control performance. Figure 13 presents the attenuation at the error microphones for the three different control conditions. More than 10 dB attenuation is achieved at three of the error microphones, when the speaker signal is used as reference. This yields a global attenuation of 8 dB in the pilot's ear level plane. When the reference signal is obtained from the accelerometer mounted on the crown panel, the error

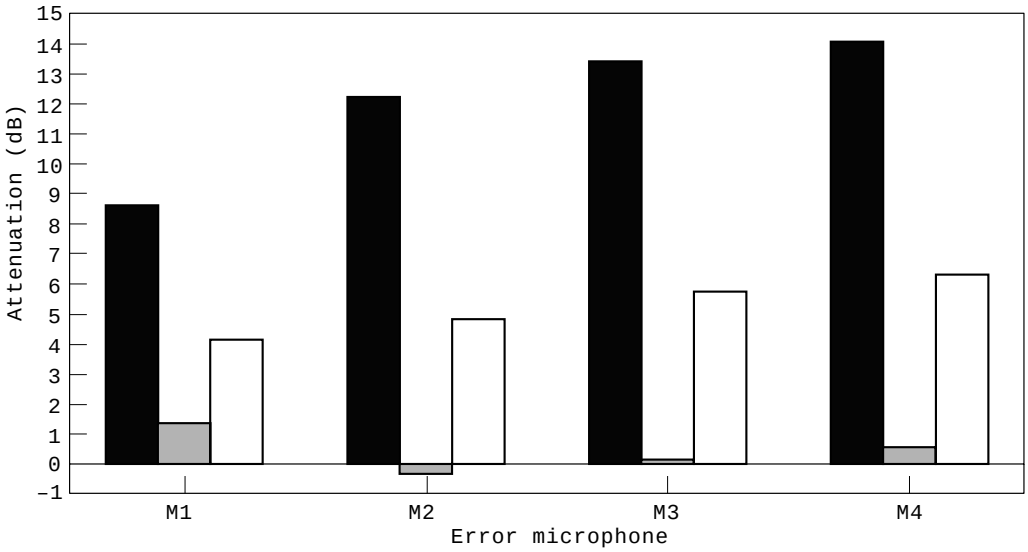


Figure 13. Attenuation at error microphones for broadband 250–1050 Hz excitation; ■, speaker as reference; ▩, accelerometer signal as reference; □, microphone signal as reference.

microphone signals are only slightly decreased. The SPL at error microphone 2 is even slightly increased in the studied frequency range. This poor performance at the error microphones leads a global SPL increase of about 1 dB in the pilot's ear level measurement plane. Using the signal from the microphone located close to the fuselage as reference signal, yields a decrease of about 5 dB in average at the error microphones. This results in a global attenuation of 3 dB in the pilot's ear level plane. Including the passive effect of the foam gives a total attenuation of about 7 dB in this case. Therefore, as the frequency bandwidth of the disturbance is increased, the short time delay for the controller to react associated with the accelerometer as reference signal, becomes critical since the signal becomes less predictable and yields a degradation of the control performance.

## 5. CONCLUSIONS

The smart skin consists of cylindrically curved PVDF piezoelectric film embedded in partially reticulated polyurethane acoustic foam. The foam-PVDF smart skin was mounted under the crown panels in the cockpit as a Cessna Citation III fuselage for performance testing (each smart foam element controlling the effective acoustic source of an individual fuselage panel). Band-limited random noise control was achieved with MIMO feedforward controller. Increasing the number of control channels (i.e., extending the smart skin to control a larger number of fuselage panels) led to an increase in global sound attenuation. Three different reference signals were also implemented for the MIMO feedforward controller. When practical reference sensors were implemented (i.e., the accelerometer and the microphone), control results are very promising. However, for all the excitation frequency bandwidths studied, control performance, when the reference signal was provided by a microphone located close the fuselage, was

much better than when the reference signal was provided by an accelerometer directly mounted on the fuselage panel. This was due to the fact that the control system was acausal, when the accelerometer signal was used as reference signal. For band-limited excitation (200 Hz bandwidth), as much as 13 dB global passive/active attenuation was achieved at the pilot's ear level, when the microphone provided the reference signal. For this reference sensor, the global passive/active attenuation is still about 7 dB when the excitation frequency bandwidth is increased to 800 Hz. Future work includes using a more complex disturbance source to excite the crown panels, as well as increasing the number of control channels to obtain a larger area of attenuation.

## ACKNOWLEDGMENTS

The authors gratefully acknowledge the support of this work by the Army Research Office under the Grant DAA H04-95-1-0037 and DARPA-ARO.

## REFERENCES

1. C. R. Fuller and J. D. Jones 1987 *Journal of Sound and Vibration* **112**(2), 389–395. Experiments on reduction of propeller induced interior noise by active control of cylinder vibration.
2. M. A. Simpson, T. M. Luong, C. R. Fuller and J. D. Jones 1991 *Journal of Aircraft* **28**(3), 208–215. Full-scale demonstration tests of cabin noise reduction using active vibration control.
3. R. J. Silcox, S. Lefebvre, V. L. Metcalf, T. B. Beyer and C. R. Fuller 1992 *AIAA* 14*th Aeroacoustics Conference*, DGLR/AIAA paper 92-2091. Evaluation of piezoceramic actuators for control of aircraft interior noise.
4. A. J. Bullmore, P. A. Nelson and S. J. Elliott 1987 *AIAA* 11*th Aeroacoustics Conference*, AIAA Paper 87-2704. Models for evaluating the performance of propeller aircraft active noise control systems.
5. U. Emborg and C. F. Ross 1993 *Second Conference on Recent Advances in Active Control of Sound and Vibration*, Blacksburg, VA, S67–S73. Active control in the SAAB 340.
6. P. A. Nelson and S. J. Elliott 1992 *Active Control of Sound*. London: Academic Press.
7. C. R. Fuller, S. J. Elliott and P. A. Nelson 1996 *Active Control of Vibration*. London: Academic Press.
8. K. W. Ng 1995 *The* 1995 *International Symposium on Active Control of Sound and Vibration*, *Active* 95, Newport Beach, CA. Applications of active control.
9. Y. J. Kang, W. Tsoi and J. S. Bolton 1993 *Proceedings of Noise-Con* 93, Williamsburg, VA, 285–290. The effect of mounting on the acoustical properties of finite-depth polyimide foam layers.
10. L. Beranek and L. Ver 1992 *Noise and Vibration Control Engineering*: *Principles and Applications*. New York: Wiley.
11. J. S. Bolton and E. R. Green 1993 *Second Conference on Recent Advances in Active Control of Sound and Vibration*, Blacksburg, VA, 139–149. Smart foams for active absorption of sound.
12. C. R. Fuller, M. J. Bronzel, C. A. Gentry and D. E. Wittington 1994 *Proceedings of Noise-Con* 94, Ft Lauderdale, FL, 429–436. Control of sound radiation/reflection with adaptive foams.

13. C. A. GENTRY, C. GUIGOU and C. R. FULLER 1997 *Journal of the Acoustical Society of America* **101**(4), 1771–1778. Smart foam for applications in passive/active noise radiation control.
14. C. R. FULLER, C. GUIGOU and C. A. GENTRY 1996 *Proceedings of SPIE's 3rd Symposium on Smart Structures and Materials*, San Diego, CA. Foam-PVDF smart skin for active control of sound.
15. C. A. GENTRY, C. GUIGOU and C. R. FULLER 1999 In preparation. Plate radiation control with smart foam.
16. POLYMER TECHNOLOGY INC. 1994 *Polymer Technology Inc.*, Newark, DE. Technical Data Sheet: acoustical products—an overview.
17. J. S. BENDAT and A. G. PIERSOL 1986 *Random Data*. New York: Wiley; second edition.